Neumann A, Wu L, Li W, Beard BL, Johnson CM, Rosso KM, Frierdich AJ, Scherer MM. Atom exchange between aqueous Fe(II) and structural Fe in clay minerals. *Environmental Science and Technology* 2015, 49(5), 2786–2795.

Atom exchange between aqueous Fe(II) and structural Fe in clay minerals

Anke Neumann,[*,†,§] Lingling Wu,[‡,∥] Weiqiang Li,[‡,⊥] Brian L. Beard,[‡] Clark M. Johnson,[‡] Kevin M. Rosso,[¶] Andrew J. Frierdich,[†,#] and Michelle M. Scherer[†]

Civil and Environmental Engineering, The University of Iowa, Iowa City, Iowa 52242, USA, Department of Geology and Geophysics, University of Wisconsin, Madison, Wisconsin 53706, USA, and Physical Sciences Division, Pacific Northwest National Laboratory, Richland, Washington 99352, USA

E-mail: anke.neumann@ncl.ac.uk

Abstract

Due to their stability towards reductive dissolution, Fe-bearing clay minerals are viewed as a renewable source of Fe redox activity in diverse environments. Recent findings of interfacial electron transfer between aqueous Fe(II) and structural Fe in clay minerals and electron conduction in octahedral sheets of nontronite, however, raise the question whether Fe interaction with clay minerals is more dynamic than previously thought. Here, we use an enriched isotope tracer approach to simultaneously and independently trace Fe atom movement from the aqueous phase to the solid (^{57}Fe) and from the solid into the aqueous phase (^{56}Fe). Over 6 months, we observed a significant

[*]To whom correspondence should be addressed [†]University of Iowa [‡]University of Wisconsin [¶]PNNL [§]Now: Civil Engineering and Geosciences, Newcastle University, Newcastle upon Tyne, NE1 7RU, UK [∥]Now: Department of Earth and Environmental Sciences, University of Waterloo, Waterloo, ON, N2L 3G1, Canada [⊥]Now: School of Earth Sciences and Engineering, Nanjing University, Nanjing, Jiangsu Province, 210046, China [#]Department of Geology and Geophysics, University of Wisconsin, Madison, Wisconsin 53706, USA

decrease in aqueous ^{57}Fe isotope fraction, with a fast initial decrease which slowed after 3 days and stabilized after about 50 days. For the aqueous ^{56}Fe isotope fraction, we observed a similar but opposite trend, indicating that Fe atom movement had occurred in both directions: from the aqueous phase into the solid and from the solid into aqueous phase. We calculated that 5–20% of structural Fe in clay minerals NAu–1, NAu–2, and SWa–1 exchanged with aqueous Fe(II), which significantly exceeds the Fe atom layer exposed directly to solution. Calculations based on electron-hopping rates in nontronite suggest that the bulk conduction mechanism previously demonstrated for hematite[1] and suggested as an explanation for the significant Fe atom exchange observed in goethite[2] may be a plausible mechanism for Fe atom exchange in Fe-bearing clay minerals. Our finding of 5–20% Fe atom exchange in clay minerals indicates that we need to rethink how Fe mobility affects the macroscopic properties of Fe-bearing phyllosilicates and its role in Fe biogeochemical cycling, as well as its use in a variety of engineered applications, such as landfill liners and nuclear repositories.

Introduction

In the earth's crust, Fe is the fourth most abundant element and reactive forms are commonly found in a variety of environments, such as atmospheric dust,[3,4] marine and fresh water bodies,[5,6] and minerals and colloids in soil and subsurface environments.[7] In these diverse environments, reactions of the Fe(II)/Fe(III) redox couple are an important driver for the cycling of many other elements, including carbon,[5,8,9] phosphorous,[10] and nitrogen.[11] In subsurface environments, Fe redox reactions often occur at mineral interfaces, including Fe (oxyhydr)oxides, sulfides, and Fe-bearing clay minerals. Although clay minerals contain a significant portion of Fe in soils,[12,13] they have mostly been regarded as sorbent phases for cations[14–18] and their Fe redox reactions have received less attention than reactions involving Fe (oxyhydr)oxides.

In the last decade, new pathways have been discovered for Fe cycling in Fe(oxyhydr)oxides

which have led to a more dynamic picture of the Fe oxide-water interface (for recent reviews see:[19,20]). Important processes at the Fe(II)-Fe oxide interface are (*i*) interfacial electron transfer between aqueous Fe(II) and mineral Fe(III),[21–23] (*ii*) bulk electron conduction within the Fe oxide mineral,[1,24] and (*iii*) Fe atom exchange between aqueous and mineral phase.[2,25,26] The first step thought to lead to extensive Fe atom cycling between aqueous and solid phase Fe is Fe(II) sorption to the mineral surface and subsequent electron transfer to the Fe (oxyhydr)oxides.[2,25,26] We recently showed that Fe(II) sorption to Fe-bearing clay minerals is also followed by electron transfer to structural Fe(III) in the clay mineral, resulting in the formation of Fe(II)-containing clay mineral and a solid Fe oxidation product.[27,28] Combined with the finding that electron conduction through the bulk of Fe-rich clay minerals is theoretically feasible at room temperature,[29] along with theoretical support for Fe(II) adsorption and electron transfer into structural Fe,[30] our recent results lead to the fascinating question of whether Fe atom exchange will also occur between aqueous Fe(II) and structural Fe in clay minerals.

Fe-containing clay minerals are typically considered more resistant towards acid dissolution compared to Fe(oxyhydr)oxides due to the greater stability provided by the silicate framework, suggesting that Fe atom exchange might be more unlikely to occur in Fe-bearing clay minerals. Dissolution during chemical reduction, a fast reaction for Fe(oxyhydr)oxides,[31] was also found to be negligible for Fe-bearing clay minerals,[32–36] whereas during microbial Fe reduction small to partial clay mineral dissolution[37–39] and even clay mineral transformation have been reported.[40] Here, we used an enriched isotope tracer approach, which we successfully applied previously to Fe oxides[2,25,26] to explore whether Fe atom exchange occurs between aqueous Fe and structural Fe in clay minerals. We determined the extent of Fe atom exchange over the course of two months for Fe-rich clay minerals NAu–1, NAu–2, and SWa–1 and studied the effects of mineral structure and reaction pH value. Experiments were carried out at two different ^{57}Fe enrichments of the aqueous Fe(II) isotope tracer to determine whether the initial isotope contrast affects Fe atom exchange.

Materials and Methods

Batch experiments

Nontronites NAu–1 (unit cell formula: $Na_{0.53}(Al_{0.15}Mg_{0.02}Fe_{1.84})(Si_{3.49}Al_{0.51})O_{10}(OH)_2$[41]) and NAu–2 (unit cell formula: $Na_{0.36}(Al_{0.17}Mg_{0.03}Fe_{1.77})(Si_{3.78}Al_{0.08}Fe_{0.15})O_{10}(OH)_2$[42]), and ferruginous smectite SWa–1 (unit cell formula: $Na_{0.43}(Al_{0.54}Mg_{0.12}Fe_{1.34})(Si_{3.69}Al_{0.31})O_{10}(OH)_2$[43]) from the Source Clays Repository of The Clay Mineral Society (www.clays.org) were subjected to a size-fractionation (<0.5 μm, SWa–1 <2 μm) and Na^+-homoionization process as described previously, to ensure delamination of clay mineral particles and remove any impurities.[27] Suspension of SWa–1 was further treated by 10 min reduction with sodium dithionite (50 mg added to 85 mg SWa–1) at 70 °C in citrate-bicarbonate buffer,[44] washed three times with anaerobic deionized water to remove aqueous Fe(II) from reduction of Fe oxide impurities, and reoxidized by bubbling with air for two full days to restore Fe(III) in SWa–1[45,46] (residual Fe(II)/Fe(tot) content of 0.4%). Batch experiments were carried out in an anaerobic glovebox (N_2/H_2: 93/7) and solutions were purged with N_2 for at least 2 hours prior to transfer into a glovebox.

A highly ^{57}Fe-enriched Fe(II) solution was prepared by dissolving metallic ^{57}Fe (>92% ^{57}Fe abundance, Isoflex, San Francisco, CA, USA) in 1 M HCl at ∼60 °C overnight, followed by dilution with deoxygenated DI water (resulting concentrations of ∼150 mM ^{57}Fe(II), ∼0.1 M HCl). A lower ^{57}Fe-enriched Fe(II) solution, which had a ^{57}Fe abundance 10% higher than the natural ^{57}Fe abundance (∼2.34% vs. ∼2.12%), was prepared by mixing the ^{57}Fe-enriched spike with a natural abundance Fe(II) solution at a molar ratio of ca. 1:500.

Batch reactors contained 15 mL of 25 mM MES (2-(N-morpholino)ethanesulfonic acid, pK_a 6.06[47]) buffer adjusted to pH 6.00±0.05 or HEPES (N-2-hydroxyethylpiperazine-N'-2-ethane-sulfonic acid, pK_a 7.55[48]) buffer adjusted to pH 7.50±0.05, 50 mM NaCl to provide constant ionic strength, and 2 mM highly ^{57}Fe-enriched or lower ^{57}Fe-enriched aqueous Fe(II). The reaction was started by adding 30.0 ± 0.2 mg of NAu–1 or NAu–2 powder to the reactor.

Experiments with SWa–1 were carried out in 5 mL of 10 mM PIPES (piperazine-N,N'-bis(2-ethanesulfonic acid), pK_a 6.8[48]) buffer adjusted to pH 6.85±0.05 and reactors contained approximately 2 mg SWa–1 (adjusted to 1 mM structural Fe) and 1 mM lower ^{57}Fe-enriched aqueous Fe(II). The resulting suspension was constantly mixed end-over-end in the dark for the pre-determined reaction time after which the reaction was stopped by centrifugation (13,000 rpm, maximum g-force 18500, 15 min). The supernatant was decanted, filtered (0.2 μm), and acidified with concentrated trace-metal grade HCl for subsequent Fe(II) and total Fe analysis according to the 1,10-phenanthroline method[49] (NAu–1, NAu–2) or the ferrozine method[50] (SWa–1) as well as for Fe isotope analysis. All experiments were carried out in triplicate (NAu–1, NAu–2) or duplicate (SWa–1) reactors.

Fe isotope analyses

Samples from experiments involving highly ^{57}Fe-enriched Fe(II) solutions were analyzed using a quadrupole inductively coupled plasma mass spectrometer (Q–ICP–MS, Thermo Fisher Scientific, X Series 2 Quadrupole) as described previously.[26] Aqueous samples were diluted in 0.1 M trace-metal grade HCl to a total Fe concentration of ∼20 ppb and spiked with 10 ppb ^{59}Co as internal standard. The spectrometer was operated in collision cell mode using H_2/ He (7/93) as collision cell gas at a flow rate of 4.2–4.5 mL/min to remove polyatomic interferences. Correction for ^{58}Ni interferences were carried out as described in the Supporting Information (SI) and was usually negligible.

Samples from experiments involving lower ^{57}Fe-enriched Fe(II) solutions, and selected samples from experiments of highly ^{57}Fe-enriched Fe(II) solutions, were analyzed using a multi collector ICP–MS (MC–ICP–MS, Micromass IsoProbe). Prior to isotope analysis, samples were purified using anion-exchange chromatography with AG-1x8 resin, 7 M HCl, and 0.5 M HCl[51,52] (details in the SI). Purified Fe was diluted to 4 ppm in 2% HNO_3 and high precision Fe isotope measurements were carried out using a standard-sample-bracketing method, against a well-characterized in-house natural abundance Fe solution. Details of

the analytical methods have been reported previously.[2,51] Analytical uncertainty (external precision) for $^{54}Fe/^{56}Fe$ and $^{57}Fe/^{56}Fe$ ratios are better than 0.02%, which is sufficient to distinguish the variability in ^{57}Fe abundance of samples in this study (initial difference in ^{57}Fe abundances between solids and solutions of ∼10%).

In the following discussions, abundance (fraction) of an Fe isotope i is denoted as f^iFe, which is calculated from signal intensities of all Fe isotopes measured by Q–ICP–MS (masses of 54, 56, 57, and 58) or measured by MC–ICP–MS (masses of 54, 56, and 57):

$$f^i\mathrm{Fe} = \frac{^i\mathrm{counts}}{^{54}\mathrm{counts} \ + \ ^{56}\mathrm{counts} \ + \ ^{57}\mathrm{counts} \ (+ \ ^{58}\mathrm{counts})} \tag{1}$$

A small offset (∼0.05) between Fe isotope fractions from Q–ICP–MS and MC–ICP–MS measurements is thus expected and will be very small due to the low natural abundance of ^{58}Fe (0.28%).

Results and Discussion

Enriched Isotope Tracer Experiment with Clay Minerals

To trace the exchange of Fe between aqueous Fe(II) and structural Fe(III) in Fe-rich clay minerals (NAu–1, NAu–2), we designed an enriched isotope Fe tracer experiment in which we could track the movement of Fe atoms in both directions, i.e., into and out of the aqueous phase, as shown in Figure 1. We reacted aqueous Fe(II) enriched in ^{57}Fe isotope (f^{57}Fe: 0.901–0.928, Tables 1, 2) and depleted in ^{56}Fe isotope (f^{56}Fe: 0.048–0.074, Tables 1, 2) with clay minerals containing Fe in its natural abundance (Q–ICP–MS measured f^{57}Fe: 0.0235 and f^{56}Fe: 0.925). By measuring changes in the relative abundance of both ^{56}Fe and ^{57}Fe isotopes in the aqueous phase, we could track Fe atom movement from the aqueous phase into the clay structure (^{57}Fe) as well as Fe atom movement from the clay structure into the aqueous phase (^{56}Fe). Measuring both isotopes allows us to simultaneously trace the

movement of Fe atoms into and out of the clay mineral. This is particularly useful when, as in our case here, substantial Fe(II) sorption to the mineral surface occurs. Mass transfer of aqueous Fe to the mineral solids biases the solid phase isotope fraction, resulting in an overestimate of the extent of atom exchange.[2,25,26,53]

Reaction of aqueous Fe(II) with NAu–1 resulted in significant loss of Fe(II) from solution (91–99%) after only several hours due to the expected sorption of Fe(II) (Table 1), which occurred predominantly to clay mineral edge OH-groups at the experimental pH value of 7.5.[14,16,17,27,54,55] In recent studies, we demonstrated that sorbed Fe(II) becomes oxidized during the electron transfer reaction to structural Fe in clay minerals and, based on Mössbauer spectroscopy and sequential extraction, that no net Fe(II) oxidation occurred in the Fe(II)/clay mineral system.[27,28] What was not anticipated, however, was the substantial and continued decrease in the fraction of aqueous ^{57}Fe over the next six months. During the first 20 days, the fraction of aqueous ^{57}Fe decreased from 0.90 to 0.71, followed by a slower decrease until after approximately 50 days, when the aqueous ^{57}Fe fraction remained at a fairly constant value of 0.60–0.65 (Table 1, Figure 1). It is important to note that mass-dependent isotope fractionation factors due to sorption of Fe(II) are very small ($\sim 1‰$),[56,57] so that uptake of Fe(II) from sorption alone would not induce any significant change in the ^{57}Fe fraction in the aqueous phase[58] and would result only in less Fe atoms in the aqueous phase, but with the same fraction of each isotope. A decrease in the fraction of ^{57}Fe indicates that aqueous ^{57}Fe was being diluted and replaced with Fe atoms of a different isotope. A similar, but opposite trend was observed for the aqueous ^{56}Fe fraction, which increased simultaneously with the decreasing aqueous ^{57}Fe fraction, indicating that the aqueous phase was becoming enriched in ^{56}Fe (Figure 1). As noted above, natural, mass-dependent fractionation caused by Fe(II) sorption[56,57] or precipitation[59–61] usually results in significantly smaller changes in isotope composition than observed with our highly ^{57}Fe-enriched aqueous Fe(II) tracer.

Concurrent dilution of aqueous ^{57}Fe and enrichment of aqueous ^{56}Fe indicates that Fe

atoms were moving into the clay mineral from the aqueous phase and, at the same time, out of the clay mineral into the aqueous phase, indicating Fe atom exchange occurred in both directions. The isotope fractions at complete mixing, $(f^i\mathrm{Fe})_{eq}$, are represented by the dashed lines in Figure 1 (for calculation see SI), which shows that only partial mixing has occurred since neither isotope reaches the mass balance calculated complete mixing fractions. Although similar atom exchange has been observed between aqueous Fe(II) and Fe oxyhydroxides[2,26,62] and Fe oxides,[25,53,63] Fe mobility into and out of a clay mineral structure is rather surprising as Fe in clay minerals is typically regarded as structurally more stable and sterically protected than in Fe oxides, consistent with the known lower susceptibility of Fe clay minerals to reductive dissolution.[35,36,39,64]

To evaluate the amount of structural Fe(III) in the clay mineral that had exchanged with aqueous Fe(II), we used a mass balance approach as described previously.[57,58] We calculated the extent of Fe atom exchange in clay minerals by:

$$percent\ clay\ mineral\ Fe\ exchange = \frac{N_{\mathrm{Fe(II)}}(f^i\mathrm{Fe(II)}_{aq}^{ini} - f^i\mathrm{Fe(II)}_{aq}^{t})}{N_{\mathrm{CM}}^{\mathrm{tot}}(f^i\mathrm{Fe(II)}_{aq}^{t} - f^i\mathrm{Fe}_{CM}^{ini})} \times 100 \qquad (2)$$

where $N_{\mathrm{Fe(II)}}$ is the number of Fe(II) atoms added to solution, $N_{\mathrm{CM}}^{\mathrm{tot}}$ is total amount of structural Fe atoms in the clay mineral, $f^i\mathrm{Fe(II)}_{aq}^{t}$ is the measured fraction of Fe isotope i in solution at each time point t, and $f^i\mathrm{Fe}_{CM}^{ini}$ and $f^i\mathrm{Fe(II)}_{aq}^{ini}$ are the measured fractions of Fe isotope i at the start of the experiment in the clay mineral and in solution, respectively. Here, we are using isotope fractions of aqueous Fe(II) as easily accessible tracers for estimating the extent of Fe atom exchange, although we acknowledge that for a comprehensive mass balance approach all Fe(II) species, including sorbed Fe(II), should be considered. Our recent assessment of the Fe(II)-goethite system, however, clearly shows that changes in isotope composition of sorbed Fe(II) suggest a greater degree of exchange than calculated from aqueous Fe(II) isotope fractions alone,[58] and thus eq 2 provides a conservative estimate

of the extent of Fe atom exchange in clay minerals. Experiments are currently underway to further evaluate the role of different clay mineral sorbed Fe(II) species in the process of Fe atom exchange.

After 3 days of reaction, roughly ∼6% of the Fe atoms in the clay mineral exchanged with the aqueous Fe(II) (Figure 2). The extent of exchange continued to increase to between 9.6% (^{57}Fe) and 9.9% (^{56}Fe) after 188 days (Table 1). The close agreement between the extent of Fe atom exchange calculated from ^{57}Fe and ^{56}Fe isotopes indicates that the mobility of Fe was both into and out of the aqueous phase. Plotting the extent of Fe atom exchange calculated from ^{56}Fe versus that from ^{57}Fe indicates an apparent stoichiometry of 1:1 (Figure S2 in the SI), providing compelling evidence that for each ^{57}Fe lost from solution, presumably to the solid phase, one ^{56}Fe atom moves into solution from the solid phase, consistent with Fe atom exchange between aqueous Fe and structural Fe in clay mineral NAu–1.

To verify the accuracy of our results from Fe isotope measurements using Q–ICP–MS, we also analyzed aqueous samples from days 35, 115, and 188 by MC–ICP–MS. Fractions of ^{57}Fe were slightly higher and ^{56}Fe slightly lower when analyzed with MC–ICP–MS compared to ^{57}Fe and ^{56}Fe fractions resulting from Q–ICP–MS measurements (filled markers in Figure 1, Table S4 in the SI). The consistent small shift of ^{57}Fe (0.032–0.085) and ^{56}Fe (0.018–0.060) fraction values between the two analysis methods resulted in very good agreement of Fe atom exchange calculated from both data sets (compare open and filled markers in Figure 2, Table S4 in the SI). The close agreement of the two data sets confirms that Fe isotope fractions measured with Q–ICP–MS can be used reliably to monitor and quantify Fe atom exchange if the initial Fe isotope contrast between aqueous and mineral Fe is large (highly enriched isotope tracer) and, due to the non-linear approach to complete isotope mixing (equation 2), for extents of Fe atom exchange of less than ∼80%.

To test whether our highly enriched tracer approach had any effect on the observed extent of Fe atom exchange, we additionally carried out experiments with aqueous Fe(II) that was enriched in ^{57}Fe to only 10% above the natural abundance of ^{57}Fe (f^{57}Fe: 0.0234,

Table 3). For experiments with NAu–1 at pH 6.0 and pH 7.5, we observed similar extents of Fe atom exchange irrespective of the initial aqueous ^{57}Fe-enrichment (compare open and filled markers in Figure S4 in the SI, Tables 1–3). The excellent agreement of the two experimental sets suggests that the initial isotopic contrast between aqueous and mineral Fe does not contribute to or even cause Fe atoms to move between solid and aqueous phase, further validating our experimental approach.

In previous studies we used solid phase characterization before and after reaction with Fe(II) to provide further evidence that Fe atom exchange occurs without solid phases changes.[2,25,26,58] In our experimental system, however, electron transfer from sorbed Fe(II) to structural Fe in the clay minerals leads to the formation of structural Fe(II) and an Fe precipitate,[27,28] such that a comparison of the (Fe) solid composition before and after the isotope experiment provides no additional evidence for Fe atom exchange between aqueous Fe(II) and structural Fe in clay minerals. It is important to note that the isotopic composition of the Fe precipitate and the initial aqueous Fe(II) is identical and, therefore, any change in isotopic composition of the aqueous phase Fe(II) is caused by Fe atom exchange with clay minerals and not with the Fe precipitate.

Effect of pH and Clay Mineral Structure on Fe Exchange

To test whether sorption of aqueous Fe(II) to edge OH-groups of clay mineral NAu–1 is a prerequisite for Fe atom exchange to occur, we carried out enriched isotope tracer experiments with NAu–1 at pH 6.0, where Fe(II) sorption to basal planes dominates.[16,17,27,54,55] Similar to the reaction of Fe(II) with NAu–1 at pH 7.5, we observed an initially fast decrease in ^{57}Fe fraction and a simultaneous increase in ^{56}Fe fraction, which plateaued after approximately 20 days (Figure S4a in the SI, Table 1). From the measured isotope fractions, we calculated that the extent of exchange reached 4.9–5.0% after 188 days (Table 1), which is lower than the extent of exchange observed at pH 7.5 but still significant given that almost all sorbed Fe(II) was located at the basal planes of NAu–1.[27] Similar trends of decreasing

^{57}Fe and increasing ^{56}Fe fractions were observed in experiments with structurally similar clay mineral NAu–2 at both pH 6.0 and 7.5 (Table 2, Figure S4b in the SI), amounting to an extent of exchange of 13.5–13.8% at pH 6.0 and 19.3–19.4% at pH 7.5 after 188 days of reaction (Figure 2, Table 2). The finding of significant Fe atom exchange between aqueous Fe(II) and both clay minerals at low and high pH values suggests that Fe atom exchange occurs irrespective of whether Fe(II) was predominantly sorbed to clay mineral basal planes or to edge OH-groups.

The consistently lower extent of Fe atom exchange observed at pH 6.0 compared to pH 7.5 suggests, however, a dependence of the extent of Fe atom exchange on the type of interaction of Fe(II) with clay minerals. Similar to the reaction between Fe(II) and Fe(III) (oxyhydr)oxides, where sorption of Fe(II) to surface OH-groups is likely the first reaction leading to Fe atom exchange, we propose that interaction of aqueous Fe(II) with surface OH-groups is crucial for Fe atom exchange to occur in clay minerals. Recent quantum mechanical calculations suggest a range of Fe(II)–clay mineral edge surface complexes bridged by hydroxyl groups are possible.[30] For both clay minerals at pH 6.0, less (reactive) sorption of aqueous Fe(II) occurs, resulting in lower extents of Fe atom exchange at pH 6.0 than at pH 7.5. Additionally, we hypothesize that the extent of Fe atom exchange depends on the extent of electron transfer to structural Fe occurring during the reaction of aqueous Fe(II) with Fe-bearing clay minerals. Because Fe atom exchange was negligible when Fe oxide hematite was reacted with aqueous Fe(III),[65] we assume that interfacial electron transfer at minerals is the first step in the Fe atom exchange reaction. The extent of Fe atom exchange between aqueous Fe(II) and clay mineral Fe(III) shows similar trends as the observed extent of electron transfer for the two clay minerals as well as pH values. Structural Fe reduction in NAu–1 was lower at pH 6.0 (2.5%) than at pH 7.5 (8.9%),[27] and the extent of electron transfer was lower for NAu–1 at pH 7.5 than for NAu–2 at pH 7.5 (16%).[28] We therefore suggest that the extent of Fe atom exchange in Fe-rich clay minerals may be correlated to the observed extent of electron transfer into the clay mineral.

Although the two clay minerals are structurally very similar and contain similar amounts of structural Fe,[41,42] NAu–1 and NAu–2 exhibit significantly different extents of Fe atom exchange and differ in their trends of Fe atom exchange. While NAu–1 underwent less Fe atom exchange (5–10%, Table 1), which reached a plateau after 20 days (Figure 2), more extensive Fe atom exchange was observed for NAu–2 (14–19%, Table 2), which continued to exchange after 20 days (Figure 2). We speculate that the extent of Fe atom exchange may be limited due to the presence of silicate sheets enclosing and stabilizing the Fe-containing octahedral sheet, which may limit the extent of reductive dissolution and/or oxidative growth before disintegration of the clay mineral structure. The presence of tetrahedral Fe in clay mineral NAu–2 may facilitate Fe atom exchange beyond the extent possible for a clay mineral containing only octahedral Fe such as NAu–1.

To test the hypothesis that the absence of tetrahedral Fe in Fe-rich clay minerals may limit the extent of Fe atom exchange, we monitored Fe atom movement between aqueous and solid phase for the widely studied ferruginous smectite SWa–1, which contains Fe only in the octahedral sheet. For the reaction around pH 7, we observed a similar trend of Fe atom exchange in SWa–1 and NAu–1 (Figure 2, Figure S3), with a maximum extent of Fe atom exchange of 10% for SWa–1 after 28 days, consistent with our hypothesis. The observed very close agreement is all the more surprising as SWa–1 and NAu–1 differ significantly in their octahedral Fe occupancy (67% and 92% of the octahedral cations are Fe, respectively), suggesting that Fe atom exchange is more strongly affected by the location of Fe in the structure of Fe-rich clay minerals compared to the effect of octahedral Fe content. However, the initial ratio of aqueous Fe(II) to solid Fe ratio was notably different (SWa–1 1:1; NAu–1 1:4) as was the particle size fraction used in the experiments (SWa–1: $< 2\ \mu m$; NAu-1: $< 0.5\ \mu m$), which may both affect Fe atom exchange. Larger particles exhibit less extensive Fe atom exchange[58] and we would expect that higher initial aqueous Fe(II) loading would result in higher extent of Fe atom exchange. The combination of these two opposing effects may possibly have led to a negligible net effect in our experiments.

How Does Exchange Occur?

In our experiments, we observed Fe atom exchange ranging from only 5% in NAu–1 at pH 6.0 up to 20% in NAu–2 at pH 7.5 (Tables 1, 2). Dynamic mixing of 20% of structural Fe in a clay mineral with aqueous Fe at room temperature is quite surprising and not what one would expect given the relative stability of these minerals. To provide some perspective on the extent of mixing, we used the unit cell parameters of NAu–1 and NAu–2 to estimate a "depth" of particle that would need to be mobilized to account for the observed 5–20% mixing based on the isotope data. From the molecular formulae of NAu–1 and NAu–2, we calculated approximate *a*- and *b*-parameters of the dioctahedral unit cell in NAu–1 and NAu–2 to be $a = 4.99$ Å and $b = 8.65$ Å (calculations and illustration in the SI[66]). Because the *c*-parameter describes the thickness of the clay mineral platelet consisting of one Fe-containing octahedral sheet enclosed by two silicate tetrahedral sheets, the *c*-dimension is irrelevant for the estimation of octahedral unit cell numbers in a clay mineral particle. A clay mineral particle of 0.5×0.5 μm (in *a*- and *b*-direction) would thus contain approximately 588 000 unit cells with around 3160 unit cells comprising the circumference of the clay mineral particle. Since Fe comprises 92% and 90% of octahedral cations in NAu–1 and NAu–2, respectively, we can assume for our calculation that octahedral unit cells contain only Fe atoms (and one octahedral vacancy each). In order for 5% of the Fe atoms to exchange, the equivalent of 9 unit cells would need to be mobilized, or 46–80 Å into the clay mineral particle, assuming Fe atom exchange occurred from the octahedral edge surfaces inward. However, for smaller particles of 0.05×0.05 μm, the penetration depth would be only 1 unit cell or 8–14 Å, suggesting that Fe atoms exposed directly to solution could potentially account for the observed 5% Fe atom exchange. In contrast, for Fe atom exchange of 10% (NAu–1, pH 7.5) or even 20% (NAu–2, pH 7.5) to occur in 0.5×0.5 μm particles, Fe atoms in 19 (NAu–1) or 37 (NAu–2) unit cells inward into the clay mineral particle, corresponding to 93–116 Å or 186–322 Å, would need to have exchanged. Also for smaller particles of 0.05×0.05 μm, the penetration depth would be at least 2–3 unit cells, indicating that "depth" of Fe atom mixing

went well beyond the Fe atom layer exposed directly to solution. Because octahedral places in SWa–1 are filled to only 67% with Fe, Fe atoms in even more unit cells would have to exchange for SWa–1 to reach the same extent of Fe atom exchange and estimates for the "depth" of mobilization for NAu–1 and NAu–2 are thus conservative measures for SWa–1.

How exchange between aqueous Fe(II) and structural Fe in clay minerals occurs is an intriguing question. For Fe oxides and oxyhydroxides, three possible mechanisms have been proposed to account for the observed Fe atom exchange between aqueous and the bulk structural Fe:[1,2,25,26,53,67] Fe diffusion through mineral pores, Fe atom diffusion within the crystal lattice, and electron conduction connecting spatially separated oxidative growth and reductive dissolution of the Fe mineral. In the case of goethite, solid-state Fe atom diffusion was ruled out as a potential mechanism to explain Fe atom mixing as the diffusion coefficients are very small and at room temperature millions of years would be required to observe the extent of Fe atom exchange that occurred over 10 days.[2,67] The recent observation of nanopores in hematite[68] suggests that internal mineral surfaces might be accessible for reaction with dissolved Fe(II)[69,70] and thus available for Fe atom exchange between aqueous and solid phase.[71] A mechanism of Fe atom exchange involving pore diffusion, however, is difficult to reconcile with the surface-site specific morphological changes observed during Fe(II)-catalyzed recrystallization of hematite,[1] as well as the absence of any morphological changes in the case of goethite.[2] At this time, the most plausible mechanism involves conduction through the bulk mineral linking spatially separated sites as demonstrated for large hematite crystals.[1] Based on the observed bulk electron conduction in hematite and extensive Fe atom mixing between aqueous Fe(II) and Fe(III) in goethite, we have proposed a "redox-driven conveyor belt" model for the Fe(II)-catalyzed recrystallization of Fe (oxyhydr)oxides. The model involves oxidative sorption of Fe(II) to one surface of the Fe (oxyhydr)oxide followed by electron transfer to Fe(III) in the Fe (oxyhydr)oxide and bulk conduction through the Fe (oxyhydr)oxide lattice, leading to reductive dissolution at a spatially different surface of the Fe (oxyhydr)oxide.[2] In the case of magnetite, this bulk conduction model may also account

in part or in full for the observed Fe atom exchange. The presence of structural vacancies in magnetite, however, together with calculated Fe atom diffusion on the order of hours to days, make Fe atom diffusion a similarly plausible mechanism.[25]

For delaminated clay minerals as in our experiments, the presence of mineral pores is unlikely because individual phyllosilicate layers are only 4.3–6.5 Å in height,[66] suggesting that an Fe exchange mechanism based on pore diffusion is improbable. Proton diffusion in clay minerals has been studied at high temperatures[72] and extrapolation to temperatures lower than 100 °C gave estimates for the diffusion coefficient at room temperature ranging between 10^{-19} cm^2 s^{-1} for montmorillonite to 10^{-21} cm^2 s^{-1} for kaolinite.[73] Assuming, for the moment, that the diffusion coefficient of Fe cations is of similar magnitude in our clay minerals as well, we estimate that the time to reach 10% and 20% Fe atom exchange in 0.5 μm particles is 3 months to 80 years (10%) and 1–328 years (20%) whereas for 0.05 μm particles the timescale is 1 day to 7 months (10%) and 3 days to 2 years (20%) (Figure S5, Table S2). The wide range of estimated time spans makes it difficult to assess the viability of Fe atom diffusion as a possible mechanism. However, Fe diffusion coefficients in nontronite are likely to be much smaller than those of protons because of larger size, mass, and charge. While in the absence of measured values a diffusion mechanism cannot be eliminated, it is a highly unlikely explanation for the observed atom exchange behavior in our system.

Results from a recent molecular modeling study provide some support for conduction as a viable mechanism. Specifically, the Fe(II)-to-Fe(III) electron hopping frequency within the octahedral sheet of nontronites was found to be significant at room temperature (10^5 s^{-1}).[29] From the one dimensional random walk model,[74] this equates to an electron diffusion coefficient of approximately 10^{-11} cm^2 s^{-1}, many orders of magnitude larger than the Fe cation diffusion coefficients discussed above. Using this diffusion coefficient, an electron hopping along the Fe-containing octahedral sheet of nontronite could travel the width of the 0.5 μm clay mineral particles in about four minutes in our experiments. Because the length of 0.5 μm is the upper limit for our size-fractionated clay minerals (NAu–1, NAu–2), shorter

distances between sites along edges are more probable.

Electrons injected by sorbed Fe(II), likely mediated by bridging OH-groups at particle edges,[27,30] would contribute to atom mixing by oxidative addition of aqueous Fe. The injected electrons would then travel within the octahedral sheet and lead to partner reductive dissolution of remote octahedral Fe close to energetically predisposed clay mineral edge surfaces, resulting in the 1:1 Fe atom mixing observed in our experiments. Thus, bulk electron conduction through the octahedral sheet appears to be a plausible mechanism to connect Fe(II) oxidation at one surface site of clay minerals NAu–1 and NAu–2 with reductive dissolution of structural Fe(III) at a spatially separated surface, within the time frame of our experiments.

Environmental Implications of Fe Mixing in Clay Minerals

Our finding of significant Fe atom exchange between aqueous Fe and structural Fe in clay minerals at room temperature indicates that Fe in clay minerals is more labile than previously thought.[32–36] With up to one fifth of structural Fe in a clay mineral exchanging with the aqueous phase without disintegration of the clay mineral structure, we need to rethink how Fe mobility affects the macroscopic properties of Fe-bearing phyllosilicates. For example, the macroscopic stability of clay minerals compared to Fe (oxyhyrd)oxides has led to wide-spread use of clay minerals in containment applications such as liner material for landfills[75,76] or in nuclear repositories.[77–79]

For confinement purposes, the crucial properties of clay mineral lining or backfill material are low hydraulic conductivity as well as high cation exchange capacities,[76–78] which are strongly affected by the redox state of structural Fe in clay minerals.[36,39,80–83] In landfill or nuclear repository settings, clay minerals are exposed to reducing conditions and the seepage water often also contains Fe(II) that is produced from reductive dissolution of Fe(oxyhydr)oxides or corrosion of storage steel canisters, conditions that are similar to those tested in our experiments. Consequently, we expect that Fe atom exchange also occurs in

Fe-bearing clay minerals in landfill liners or nuclear repositories, rendering the phyllosilicate framework less stable on a microscopic level and possibly leading to altered hydraulic conductivity as well as cation exchange properties. These changes may result in deteriorating containment of stored waste and increased leakage.

Our finding of Fe mobility between aqueous phase and clay minerals also has implications well beyond current day environmental concerns. For example, the cycling of Fe in Fe-bearing clay minerals raises the question of whether Fe-bearing clay minerals' isotopic signatures can be used to interpret the ancient rock record since their isotopic signature may be altered by changes in redox conditions. Fe(II)-containing clay minerals have also been suggested to play a role in the origin of life.[84,85] For example, a recent study emphasized the predominant formation of Fe-rich clay minerals such as nontronite during the cooling of early earth's crust and suggested that, due to the absence of oxygen in early earth's atmosphere, Fe(II)-containing clay minerals may have determined the reactivity at the mineral-water interface.[86] It has been hypothesized that the reactive surfaces of clay minerals may have acted as templates and reactive catalysts for pre-biotic molecule synthesis during earth's early history, and perhaps the dynamic exchange of Fe observed here played some role in their ability to catalyze or template pre-biotic molecules in primordial times.

Acknowledgement

Funding for this work was provided from the U.S. Department of Energy Office of Biological and Environmental Research's Subsurface Biogeochemical Research (SBR) grant no. DE-SC0006692 (MMS, BLB, CMJ, and KMR); from the Swiss National Science Foundation grant no. PBEZP2_137292 (AN), and from the German Research Foundation grant no. NE 1715/1-1 (AN). KMR was also supported by the SBR Science Focus Area program at PNNL. AJF received support from the National Science Foundation under Award No. EAR-PF 1347848.

Supporting Information Available

Supporting information contains details on the calculations of the depth of Fe atom exchange and of the time scale for Fe atom diffusion within clay minerals; additional figures of isotope fractions measured during the reaction of NAu–1 and NAu–2 at pH 6.0 and pH 7.5 with high and low (NAu–1 only) ^{57}Fe(II)-enriched aqueous Fe(II) and of the extent of exchange calculated from ^{54}Fe, ^{56}Fe, and ^{57}Fe isotope fractions; and an additional table comparing isotope data acquired with Q–ICP–MS and MC–ICP–MS. This material is available free of charge via the Internet at `http://pubs.acs.org/`.

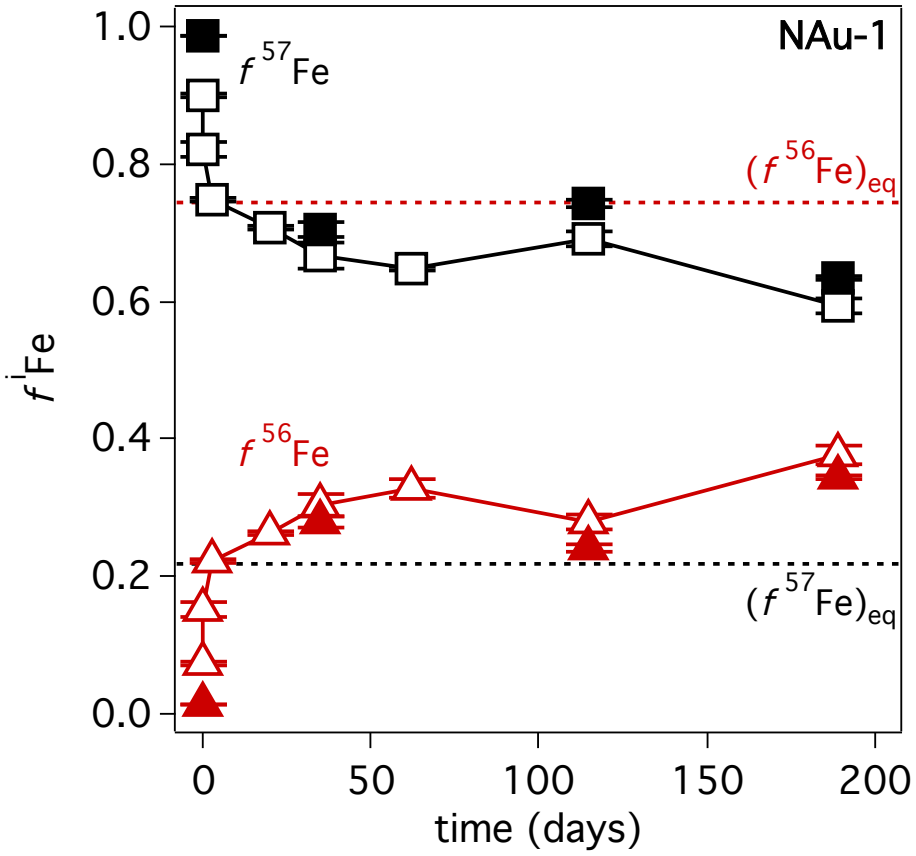

Figure 1: Fractions of ^{57}Fe (black) and ^{56}Fe (red) in the aqueous phase at pH 7.5 during the reaction of aqueous Fe(II) enriched in ^{57}Fe and depleted in ^{56}Fe with clay mineral NAu–1 containing ^{57}Fe and ^{56}Fe in their natural abundance. Good agreement of isotope measurements with a quadrupole inductively coupled mass spectrometer (Q–ICP–MS, open markers) and with a multi-collector ICP–MS (MC–ICP–MS, filled markers) were achieved. Dashed lines indicate the calculated isotope equilibrium fraction for ^{57}Fe (black) and ^{56}Fe (red). For calculation of the dashed lines representing the Fe isotope fractions at isotopic equilibrium ($(f^{i}\text{Fe})_{eq}$), see SI.

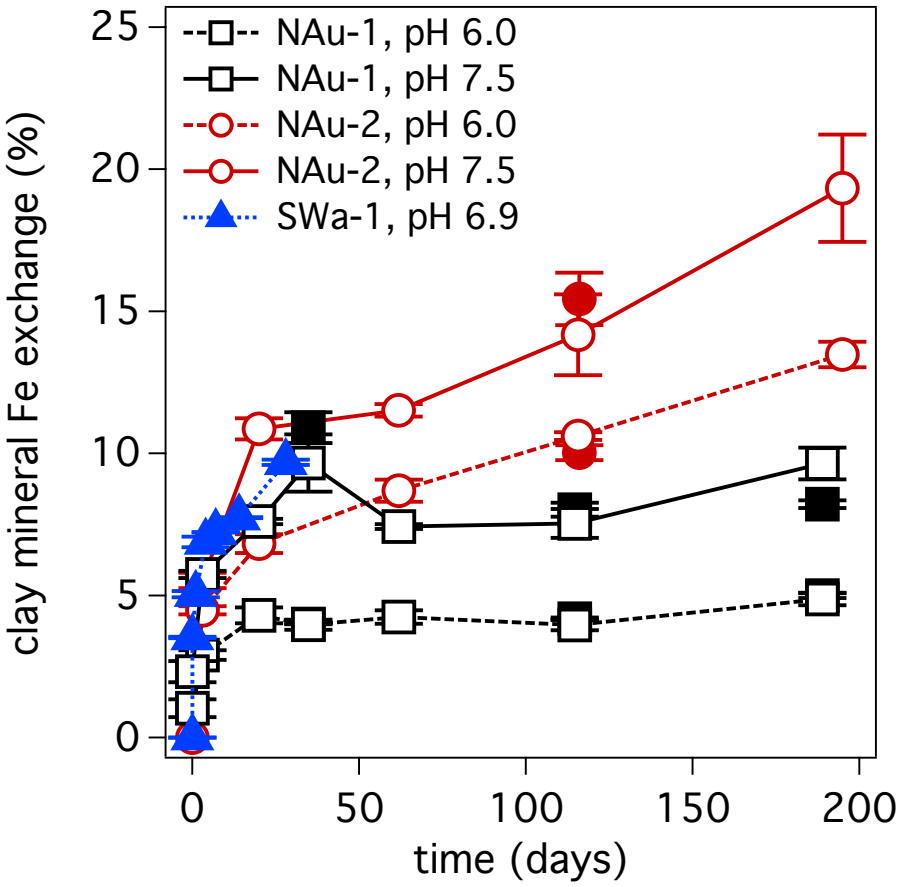

Figure 2: Extent of Fe isotope exchange between aqueous Fe(II) and structural Fe in clay minerals NAu–1 (black squares) and NAu–2 (red circles) at pH 6.0 (dashed line) and pH 7.5 (solid line), and in clay mineral SWa–1 at pH 6.9 (blue triangles), calculated from aqueous phase ^{57}Fe according to equation 2. Fe atom exchange was calculated from isotope fractions measured with a quadrupole inductively coupled mass spectrometer (Q–ICP–MS, open markers) and with a multi-collector ICP–MS (MC–ICP–MS, filled markers). Experiments were carried out with aqueous Fe(II) highly enriched in ^{57}Fe (NAu–1, NAu–2) and with low ^{57}Fe-enriched aqueous Fe(II) (SWa–1).

Table 1: Aqueous phase Fe mass and isotope data for the reaction of aqueous Fe(II) with clay mineral NAu–1 at pH 6.0 and pH 7.5. Numbers in parentheses are standard deviations from analysis of triplicate reactors.

time	**initial Fe(II)$_{aq}$**	**final Fe(II)$_{aq}$**	**sorbed Fe(II)[a]**		**f^{57}Fe**	**exchange ^{57}Fe**	**f^{56}Fe**	**exchange ^{56}Fe**	**f^{54}Fe**	**exchange ^{54}Fe**
days	μmol	μmol	μmol	%		%		%	%	
pH 6.0										
0	–	–	–	–	0.928(0.003)	0	0.048(0.003)	0	0.0032(0.0002)	0
0.04	29.9(3.1)	20.3(0.4)	9.6(3.5)	32	0.893(0.010)	1.0(0.3)	0.084(0.010)	1.1(0.3)	0.0052(0.0005)	1.2(0.3)
3	32.3(0.2)	17.6(0.3)	14.6(0.5)	45	0.840(0.005)	2.9(0.2)	0.133(0.005)	2.9(0.2)	0.0078(0.0000)	3.0(0.0)
20	35.3(0.3)	25.3(0.3)	10.0(0.6)	28	0.813(0.007)	4.3(0.3)	0.161(0.006)	4.4(0.3)	0.0088(0.0005)	4.2(0.4)
35	31.3(0.1)	22.5(0.1)	8.8(0.2)	28	0.808(0.005)	4.0(0.2)	0.165(0.004)	4.0(0.2)	0.0089(0.0004)	3.8(0.3)
62	21.8(0.1)	12.2(0.0)	9.6(0.1)	44	0.757(0.008)	4.2(0.2)	0.214(0.008)	4.2(0.2)	0.0118(0.0004)	4.3(0.2)
115	30.6(0.7)	18.1(0.4)	12.5(1.1)	41	0.806(0.005)	4.0(0.2)	0.167(0.004)	4.0(0.2)	0.0088(0.0000)	3.6(0.0)
189	21.2(0.2)	9.9(4.4)	11.4(4.5)	54	0.731(0.007)	4.9(0.2)	0.241(0.007)	5.0(0.2)	0.0110(0.0004)	3.7(0.2)
pH 7.5										
0	–	–	–	–	0.901(0.004)	0	0.074(0.004)	0	0.0056(0.0007)	0
0.04	27.9(0.1)	2.46(0.06)	25.5(0.2)	91	0.822(0.011)	2.3(0.4)	0.152(0.011)	2.4(0.4)	0.0092(0.0007)	2.1(0.4)
3	32.5(0.5)	0.65(0.00)	31.9(0.5)	98	0.748(0.003)	5.7(0.1)	0.223(0.003)	5.8(0.1)	0.0123(0.0002)	5.0(0.1)
20	32.1(0.4)	1.25(0.25)	30.9(0.5)	96	0.707(0.002)	7.6(0.1)	0.263(0.002)	7.6(0.1)	0.0149(0.0003)	7.4(0.3)
35	32.0(0.5)	0.62(0.03)	31.3(0.5)	98	0.666(0.018)	9.7(1.0)	0.303(0.017)	9.7(1.0)	0.0166(0.0009)	9.1(0.9)
62	22.2(0.1)	0.60(0.00)	21.6(0.1)	97	0.648(0.002)	7.4(0.1)	0.327(0.013)	7.8(0.6)	0.0178(0.0004)	7.3(0.3)
115	28.7(0.4)	0.36(0.02)	28.4(0.4)	99	0.691(0.011)	7.5(0.5)	0.280(0.010)	7.6(0.5)	0.0147(0.0008)	6.5(0.7)
188	21.5(0.7)	0.47(0.03)	21.0(0.7)	98	0.593(0.012)	9.6(0.6)	0.377(0.014)	9.9(0.7)	0.0175(0.0007)	6.8(0.5)

[a] Sorbed Fe(II) was calculated as the difference between initial Fe(II)$_{aq}$ and final Fe(II)$_{aq}$.

Table 2: Aqueous phase Fe mass and isotope data for the reaction of aqueous Fe(II) with clay mineral NAu–2 at pH 6.0 and pH 7.5. Numbers in parentheses are standard deviations from analysis of triplicate reactors.

time	**initial $Fe(II)_{aq}$**	**final $Fe(II)_{aq}$**	**sorbed Fe(II)[a]**		f^{57}**Fe**	**exchange ^{57}Fe**	f^{56}**Fe**	**exchange ^{56}Fe**	f^{54}**Fe**	**exchange ^{54}Fe**
days	μmol	μmol	μmol	%		%		%	%	
pH 6.0										
0	–	–	–	–	0.928(0.003)	0	0.048(0.003)	0	0.0032(0.0002)	0
3	32.3(0.2)	13.5(0.3)	18.8(0.5)	58	0.799(0.003)	4.5(0.1)	0.173(0.003)	4.5(0.1)	0.0101(0.0003)	4.9(0.2)
20	35.5(0.2)	18.0(0.1)	17.5(0.3)	49	0.759(0.007)	6.8(0.3)	0.214(0.006)	6.9(0.3)	0.0132(0.0028)	6.7(0.1)
62	35.5(0.1)	15.8(0.2)	19.7(0.4)	55	0.722(0.007)	8.7(0.4)	0.249(0.048)	8.8(0.4)	0.0132(0.0006)	8.4(0.6)
116	35.5(0.1)	11.0(0.4)	24.5(0.5)	69	0.689(0.002)	10.6(0.1)	0.281(0.001)	10.7(0.1)	0.0151(0.0001)	10.6(0.2)
195	21.4(0.2)	6.4(0.2)	15.0(0.4)	70	0.537(0.007)	13.5(0.4)	0.432(0.008)	13.8(0.5)	0.0232(0.0006)	14.1(0.7)
pH 7.5										
0	–	–	–	–	0.901(0.004)	0	0.074(0.004)	0	0.0056(0.0007)	0
3	32.5(0.5)	0.65(0.03)	31.8(0.5)	98	0.752(0.006)	5.5(0.3)	0.223(0.003)	5.5(0.3)	0.0121(0.0003)	4.9(0.3)
20	32.1(0.4)	0.80(0.04)	31.3(0.4)	98	0.646(0.006)	10.9(0.4)	0.321(0.006)	10.9(0.4)	0.0180(0.0006)	10.8(0.7)
63	29.9(0.1)	0.38(0.04)	29.6(0.1)	99	0.624(0.004)	11.5(0.2)	0.345(0.003)	11.6(0.2)	0.0180(0.0001)	10.2(0.2)
116	29.9(0.1)	0.38(0.04)	29.6(0.1)	99	0.583(0.020)	14.2(1.4)	0.384(0.020)	14.3(1.4)	0.0204(0.0015)	13.2(2.0)
195	21.3(0.1)	0.27(0.01)	21.1(0.1)	99	0.445(0.021)	19.3(1.9)	0.517(0.022)	19.4(2.0)	0.0284(0.0006)	20.2(1.1)

[a] Sorbed Fe(II) was calculated as the difference between initial $Fe(II)_{aq}$ and final $Fe(II)_{aq}$.

Table 3: Aqueous phase Fe mass and isotope data for the reaction of low ^{57}Fe-enriched aqueous Fe(II) with clay mineral NAu–1 at pH 6.0 and 7.5, and clay mineral SWa–1 at pH 6.9. Numbers in parentheses are standard deviations from analysis of triplicate reactors.

time	**initial Fe(II)$_{aq}$**	**final Fe(II)$_{aq}$**	**sorbed Fe(II)[a]**		**f^{57}Fe**	**exchange ^{57}Fe**	**f^{56}Fe**	**exchange ^{56}Fe**
days	μmol	μmol	μmol	%		%		%
NAu–1, pH 6.0								
0	–	–	–	–	0.023424[b]	0	0.918058[b]	0
30	34.7(0.1)	24.3(0.5)	10.4(0.6)	30	0.023180(0.000025)	3.6(0.4)	0.918631(0.000054)	3.4(0.4)
57	34.7(0.1)	24.7(0.3)	10.0(0.4)	29	0.023155(0.000003)	4.0(0.1)	0.918517(0.000132)	3.7(0.0)
NAu–1, pH 7.5								
0	–	–	–	–	0.023424[b]	0	0.918058[b]	0
30	34.6(0.3)	0.74(0.06)	33.9(0.4)	98	0.022818(0.000057)	11.1(1.4)	0.918631(0.000054)	10.7(1.4)
57	34.6(0.3)	0.73(0.01)	33.9(0.3)	98	0.022936(0.000142)	8.4(3.1)	0.918517(0.000132)	8.1(2.9)
SWa–1, pH 6.9								
0	–	–	–	–	0.023594(0.000000)	0	0.917923(0.000000)	0
0.003	5.00(0.25)[c]	4.57(0.00)	0.43(0.00)	9	0.023515(0.000001)	3.5(0.0)	0.917994(0.000000)	3.3(0.0)
1	5.00(0.25)[c]	4.47(0.01)	0.53(0.01)	11	0.023482(0.000002)	5.1(0.1)	0.918010(0.000003)	4.0(0.1)
4	5.00(0.25)[c]	4.27(0.00)	0.73(0.00)	15	0.023443(0.000004)	6.9(0.2)	0.918046(0.000003)	5.8(0.2)
7	5.00(0.25)[c]	4.36(0.04)	0.64(0.04)	13	0.023436(0.000000)	7.2(0.0)	0.918056(0.000004)	6.3(0.2)
14	5.00(0.25)[c]	4.27(0.00)	0.73(0.00)	15	0.023426(0.000000)	7.7(0.0)	0.918068(0.000002)	6.9(0.1)
28	5.00(0.25)[c]	4.07(0.08)	0.93(0.08)	19	0.023388(0.000002)	9.7(0.1)	0.918107(0.000000)	8.9(0.0)

[a] Sorbed Fe(II) was calculated as the difference between initial Fe(II)$_{aq}$ and final Fe(II)$_{aq}$.

[b] One aqueous sample was analyzed for the initial isotope composition; 95% confidence interval of the measured isotope ratios was less than 10%.

[c] 5% error from ferrozine analysis

References

(1) Yanina, S. V.; Rosso, K. M. Linked reactivity at mineral-water interfaces through bulk crystal conduction. *Science* **2008**, *320*, 218–222.

(2) Handler, R. M.; Beard, B. L.; Johnson, C. M.; Scherer, M. M. Atom Exchange between Aqueous Fe(II) and Goethite: An Fe Isotope Tracer Study. *Environ. Sci. Technol.* **2009**, *43*, 1102–1107.

(3) Achterberg, E. P.; Mark Moore, C.; Henson, S. A.; Steigenberger, S.; Stohl, A.; Eckhardt, S.; Avendano, L. C.; Cassidy, M.; Hembury, D.; Klar, J. K.; Lucas, M. I.; Macey, A. I.; Marsay, C. M.; Ryan-Keogh, T. J. Natural iron fertilization by the Eyjafjallajökull volcanic eruption. *Geophys Res Lett* **2013**, *40*, 921–926.

(4) Schulz, M.; Prospero, J. M.; Baker, A. R.; Dentener, F.; Ickes, L.; Liss, P. S.; Mahowald, N. M.; Nickovic, S.; Garcia-Pando, C. P.; Rodriguez, S.; Sarin, M.; Tegen, I.; Duce, R. A. Atmospheric Transport and Deposition of Mineral Dust to the Ocean: Implications for Research Needs. *Environ. Sci. Technol.* **2012**, *46*, 10390–10404.

(5) Lalonde, K.; Mucci, A.; Ouellet, A.; Gelinas, Y. Preservation of organic matter in sediments promoted by iron. *Nature* **2012**, *483*, 198–200.

(6) von der Heyden, B. P.; Roychoudhury, A. N.; Mtshali, T. N.; Tyliszczak, T.; Myneni, S. C. B. Chemically and Geographically Distinct Solid-Phase Iron Pools in the Southern Ocean. *Science* **2012**, *338*, 1199–1201.

(7) Stumm, W.; Sulzberger, B. The cycling of iron in natural environments: Considerations based on laboratory studies of heterogeneous redox processes. *Geochim. Cosmochim. Acta* **1992**, *56*, 3233–3257.

(8) Nealson, K. H.; Myers, C. R. Microbial reduction of manganese and iron - new approaches to carbon cycling. *Appl. Environ. Microbiol.* **1992**, *58*, 439–443.

(9) Smetacek, V. et al. Deep carbon export from a Southern Ocean iron-fertilized diatom bloom. *Nature* **2012**, *487*, 313–319.

(10) Murray, G. C.; Hesterberg, D. Iron and phosphate dissolution during abiotic reduction of ferrihydrite-boehmite mixtures. *Soil Sci. Soc. Am. J.* **2006**, *70*, 1318–1327.

(11) Li, Y.; Yu, S.; Strong, J.; Wang, H. Are the biogeochemical cycles of carbon, nitrogen, sulfur, and phosphorus driven by the "Fe^{III}–Fe^{II} redox wheel" in dynamic redox environments? *J. Soil. Sediment* **2012**, *12*, 683–693.

(12) Amonette, J. E. In *Electrochemical Properties of Clays*; Fitch, A., Ed.; CMS Workshop Lectures; The Clay Minerals Society: Aurora, CO, 2002; Vol. 10; pp 89–146.

(13) Murad, E.; Fischer, W. R. The geobiochemical cycle of iron. *NATO ASI Ser., Ser. C* **1988**, *217, Iron in Soils and Clay Minerals*, 1–18, Stucki, J. W., B. A. Goodman and U. Schwertmann (Ed.).

(14) Bradbury, M. H.; Baeyens, B. A mechanistic description of Ni and Zn sorption on Na-montmorillonite. 2. Modeling. *J. Contam. Hydrol.* **1997**, *27*, 223–248.

(15) Bradbury, M. H.; Baeyens, B. Sorption modelling on illite Part I: Titration measurements and the sorption of Ni, Co, Eu and Sn. *Geochim. Cosmochim. Acta* **2009**, *73*, 990–1003.

(16) Charlet, L.; Schindler, P. W.; Spadini, L.; Furrer, G.; Zysset, M. Cation adsorption on oxides and clays - the aluminum case. *Aquat. Sci.* **1993**, *55*, 291–303.

(17) Fletcher, P.; Sposito, G. The chemical modeling of clay electrolyte interactions for montmorillonite. *Clay Miner.* **1989**, *24*, 375–391.

(18) Schlegel, M. L.; Charlet, L.; Manceau, A. Sorption of metal ions on clay minerals - II. Mechanism of Co sorption on hectorite at high and low ionic strength and impact on the sorbent stability. *J. Colloid Interface Sci.* **1999**, *220*, 392–405.

(19) Gorski, A., Christopher; Scherer, M., Michelle *Aquatic Redox Chemistry*; ACS Symposium Series; American Chemical Society, 2011; Vol. 1071; pp 315–343.

(20) Latta, D. E.; Gorski, C. A.; Scherer, M. M. Influence of Fe^{2+}-catalysed iron oxide recrystallization on metal cycling. *Biochem. Soc. T.* **2012**, *40*, 1191–1197, 6.

(21) Gorski, C. A.; Scherer, M. M. Influence of Magnetite Stoichiometry on Fe^{II} Uptake and Nitrobenzene Reduction. *Environ. Sci. Technol.* **2009**, *43*, 3675–3680.

(22) Larese-Casanova, P.; Scherer, M. M. Fe(II) sorption on hematite: New insights based on spectroscopic measurements. *Environ. Sci. Technol.* **2007**, *41*, 471–477.

(23) Williams, A. G. B.; Scherer, M. M. Spectroscopic evidence for Fe(II)–Fe(III) electron transfer at the iron oxide-water interface. *Environ. Sci. Technol.* **2004**, *38*, 4782–4790.

(24) Rosso, K. M.; Yanina, S. V.; Gorski, C. A.; Larese-Casanova, P.; Scherer, M. M. Connecting Observations of Hematite (α-Fe_2O_3) Growth Catalyzed by Fe(II). *Environ. Sci. Technol.* **2010**, *44*, 61–67.

(25) Gorski, C. A.; Handler, R. M.; Beard, B. L.; Pasakarnis, T.; Johnson, C. M.; Scherer, M. M. Fe Atom Exchange between Aqueous Fe^{2+} and Magnetite. *Environ. Sci. Technol.* **2012**, *46*, 12399–12407.

(26) Latta, D. E.; Bachman, J. E.; Scherer, M. M. Fe Electron Transfer and Atom Exchange in Goethite: Influence of Al-Substitution and Anion Sorption. *Environ. Sci. Technol.* **2012**, *46*, 10614–10623.

(27) Neumann, A.; Olson, T. L.; Scherer, M. M. Spectroscopic evidence for Fe(II)–Fe(III) electron transfer at clay mineral edge and basal sites. *Environ. Sci. Technol.* **2013**, *47*, 6969–6977.

(28) Schaefer, M. V.; Gorski, C. A.; Scherer, M. M. Spectroscopic Evidence for Interfacial Fe(II)–Fe(III) Electron Transfer in a Clay Mineral. *Environ. Sci. Technol.* **2011**, *45*, 540–545.

(29) Alexandrov, V.; Neumann, A.; Scherer, M. M.; Rosso, K. M. Electron Exchange and Conduction in Nontronite from First-Principles. *J. Phys. Chem. C* **2013**, *117*, 2032–2040.

(30) Alexandrov, V.; Rosso, K. M. Insights into the mechanism of Fe(II) adsorption and oxidation at Fe-clay mineral surfaces from first-principles calculations. *J. Phys. Chem. C* **2013**, 22880–22886.

(31) Cornell, R. M.; Schwertmann, U. *The Iron Oxides: Structure, Properties, Reactions, Occurences and Uses.*; Wiley: Weinheim, 2003; Chapter 12, pp 297–344.

(32) Fialips, C. I.; Huo, D.; Yan, L. B.; Wu, J.; Stucki, J. W. Infrared study of reduced and reduced-reoxidized ferruginous smectite. *Clays Clay Miner.* **2002**, *50*, 455–469.

(33) Komadel, P.; Madejova, J.; Stucki, J. W. Reduction and Reoxidation of Nontronite - Questions of Reversibility. *Clays Clay Miner.* **1995**, *43*, 105–110.

(34) Neumann, A.; Petit, S.; Hofstetter, T. B. Evaluation of redox-active iron sites in smectites using middle and near infrared spectroscopy. *Geochim. Cosmochim. Acta* **2011**, *75*, 2336–2355.

(35) Ribeiro, F. R.; Fabris, J. D.; Kostka, J. E.; Komadel, P.; Stucki, J. W. Comparisons of structural iron reduction in smectites by bacteria and dithionite: II. A variable-temperature Mossbauer spectroscopic study of Garfield nontronite. *Pure Appl. Chem.* **2009**, *81*, 1499–1509.

(36) Stucki, J. W.; Golden, D. C.; Roth, C. B. Effects of reduction and reoxidation of structural iron on the surface charge and dissolution of dioctahedral smectites. *Clays Clay Miner.* **1984**, *32*, 350–356.

(37) Dong, H. L.; Kostka, J. E.; Kim, J. Microscopic evidence for microbial dissolution of smectite. *Clays Clay Miner.* **2003**, *51*, 502–512.

(38) Jaisi, D. P.; Kukkadapu, R. K.; Eberl, D. D.; Dong, H. L. Control of Fe(III) site occupancy on the rate and extent of microbial reduction of Fe(III) in nontronite. *Geochim. Cosmochim. Acta* **2005**, *69*, 5429–5440.

(39) Kostka, J. E.; Wu, J.; Nealson, K. H.; Stucki, J. W. The impact of structural Fe(III) reduction by bacteria on the surface chemistry of smectite clay minerals. *Geochim. Cosmochim. Acta* **1999**, *63*, 3705–3713.

(40) Kim, J.; Dong, H. L.; Seabaugh, J.; Newell, S. W.; Eberl, D. D. Role of microbes in the smectite-to-illite reaction. *Science* **2004**, *303*, 830–832.

(41) Keeling, J. L.; Raven, M. D.; Gates, W. P. Geology and characterization of two hydrothermal nontronites from weathered metamorphic rocks at the Uley Graphite Mine, South Australia. *Clays Clay Miner.* **2000**, *48*, 537–548.

(42) Gates, W. P.; Slade, P. G.; Manceau, A.; Lanson, B. Site occupancies by iron in nontronites. *Clays Clay Miner.* **2002**, *50*, 223–239.

(43) Manceau, A.; Lanson, B.; Drits, V. A.; Chateigner, D.; Gates, W. P.; Wu, J.; Huo, D.; Stucki, J. W. Oxidation-reduction mechanism of iron in dioctahedral smectites: I. Crystal chemistry of oxidized reference nontronites. *Am. Mineral.* **2000**, *85*, 133–152.

(44) Stucki, J. W.; Golden, D. C.; Roth, C. B. Preparation and handling of dithionite-reduced smectite suspensions. *Clays Clay Miner.* **1984**, *32*, 191–197.

(45) Komadel, P.; Lear, P. R.; Stucki, J. W. Reduction and reoxidation of nontronite - extent of reduction and reaction rates. *Clays Clay Miner.* **1990**, *38*, 203–208.

(46) Shelobolina, E. S.; Vanpraagh, C. G.; Lovley, D. R. Use of ferric and ferrous iron containing minerals for respiration by Desulfitobacterium frappieri. *Geomicrobiol. J.* **2003**, *20*, 143–156.

(47) Kandegedara, A.; Rorabacher, D. B. Noncomplexing tertiary amines as "better" buffers covering the range of pH 3-11. Temperature dependence of their acid dissociation constants. *Anal. Chem.* **1999**, *71*, 3140–3144.

(48) Good, N. E.; Winget, G. D.; Winter, W.; Connolly, T. N.; Izawa, S.; Singh, R. M. M. Hydrogen ion buffers for biological research. *Biochemistry* **1966**, *5*, 467–477.

(49) Schilt, A. A. *Applications of 1,10-phenanthroline and related compounds*, 1st ed.; Pergamon Press: Oxford, 1969.

(50) Stookey, L. Ferrozine: a new spectrophotometric reagent for iron. *Anal. Chem.* **1970**, *42*, 779–781.

(51) Beard, B. L.; Johnson, C. M.; Skulan, J. L.; Nealson, K. H.; Cox, L.; Sun, H. Application of Fe isotopes to tracing the geochemical and biological cycling of Fe. *Chem. Geol.* **2003**, *195*, 87–117.

(52) Strelow, F. W. E. Improved separation of iron from copper and other elements by anion-exchange chromatography on a 4% crosslinkage resin with high concentrations of hydrochloric acid. *Talanta* **1980**, *27*, 727–732.

(53) Crosby, H. A.; Johnson, C. M.; Roden, E. E.; Beard, B. L. Coupled Fe(II)-Fe(III) electron and atom exchange as a mechanism for Fe isotope fractionation during dissimilatory iron oxide reduction. *Environ. Sci. Technol.* **2005**, *39*, 6698–6704.

(54) Jaisi, D. P.; Liu, C. X.; Dong, H. L.; Blake, R. E.; Fein, J. B. Fe^{2+} sorption onto nontronite (NAu–2). *Geochim. Cosmochim. Acta* **2008**, *72*, 5361–5371.

(55) Schultz, C.; Grundl, T. pH Dependence of ferrous sorption onto two smectite clays. *Chemosphere* **2004**, *57*, 1301–1306.

(56) Teutsch, N.; von Gunten, U.; Porcelli, D.; Cirpka, O. A.; Halliday, A. N. Adsorption as a cause for iron isotope fractionation in reduced groundwater. *Geochim. Cosmochim. Acta* **2005**, *69*, 4175–4185.

(57) Mikutta, C.; Wiederhold, J. G.; Cirpka, O. A.; Hofstetter, T. B.; Bourdon, B.; Von Gunten, U. Iron isotope fractionation and atom exchange during sorption of ferrous iron to mineral surfaces. *Geochim. Cosmochim. Acta* **2009**, *73*, 1795–1812.

(58) Handler, R. M.; Frierdich, A. J.; Johnson, C. M.; Rosso, K. M.; Beard, B. L.; Wang, C.; Latta, D. E.; Neumann, A.; Pasakarnis, T.; Premaratne, W. A. P. J.; Scherer, M. M. Fe(II)-catalyzed recrystallization of goethite revisited. *Environ. Sci. Technol.* **2014**, *48*, 11302–11311.

(59) Bullen, T. D.; White, A. F.; Childs, C. W.; Vivit, D. V.; Schulz, M. S. Demonstration of significant abiotic iron isotope fractionation in nature. *Geology* **2001**, *29*, 699?702.

(60) Wu, L.; Beard, B. L.; Roden, E. E.; Johnson, C. M. Stable Iron Isotope Fractionation Between Aqueous Fe(II) and Hydrous Ferric Oxide. *Environ. Sci. Technol.* **2011**, *45*, 1847–1852.

(61) Welch, S. A.; Beard, B. L.; Johnson, C. M.; Braterman, P. S. Kinetic and equilibrium Fe isotope fractionation between aqueous Fe(II) and Fe(III). *Geochim. Cosmochim. Acta* **2003**, *67*, 4231–4250.

(62) Frierdich, A. J.; Beard, B. L.; Reddy, T. R.; Scherer, M. M.; Johnson, C. M. Iron isotope fractionation between aqueous Fe(II) and goethite revisited: New insights based on a multi-direction approach to equilibrium and isotopic exchange rate modification. *Geochim. Cosmochim. Acta* **2014**, *139*, 383–398.

(63) Frierdich, A. J.; Beard, B. L.; Scherer, M. M.; Johnson, C. M. Determination of the $Fe(II)_{aq}$-magnetite equilibrium iron isotope fractionation factor using the three-isotope method and a multi-direction approach to equilibrium. *Earth Planet Sc Lett* **2014**, *391*, 77–86.

(64) Ernstsen, V.; Gates, W. P.; Stucki, J. W. Microbial reduction of structural iron in clays - A renewable source of reduction capacity. *J. Environ. Qual.* **1998**, *27*, 761–766, clay.

(65) Skulan, J. L.; Beard, B. L.; Johnson, C. M. Kinetic and equilibrium Fe isotope fractionation between aqueous Fe(III) and hematite. *Geochim. Cosmochim. Acta* **2002**, *66*, 2995–3015.

(66) Meunier, A. *Clays*; Springer: Berlin, 2005; pp 1–60.

(67) Pedersen, H. D.; Postma, D.; Jakobsen, R.; Larsen, O. Fast transformation of iron oxyhydroxides by the catalytic action of aqueous Fe(II). *Geochim. Cosmochim. Acta* **2005**, *69*, 3967–3977.

(68) Echigo, T.; Monsegue, N.; Aruguete, D. M.; Murayama, M.; Hochella, M. F. Nanopores in hematite (α–Fe_2O_3) nanocrystals observed by electron tomography. *Am. Mineral.* **2013**, *98*, 154–162.

(69) Fischer, L.; Bruemmer, G. W.; Barrow, N. J. Observations and modelling of the reactions of 10 metals with goethite: adsorption and diffusion processes. *Eur. J. Soil Sci.* **2007**, *58*, 1304–1315.

(70) Mikutta, C.; Lang, F.; Kaupenjohann, M. Citrate impairs the micropore diffusion of phosphate into pure and C-coated goethite. *Geochim. Cosmochim. Acta* **2006**, *70*, 595–607.

(71) Putnis, A. Mineral replacement reactions: from macroscopic observations to microscopic mechanisms. *Mineral. Mag.* **2002**, *66*, 689–708.

(72) Cole, D. R.; Ohmoto, H. Kinetics of isotopic exchange at elevated temperatures and pressures. *Rev. Mineral.* **1986**, *16*, 41–90.

(73) Kyser, T. K.; Kerrich, R. In *Stable Isotope Geochemistry: A Tribute to Samuel Epstein*; Taylor, H. P., O'Neil, J. R., Kaplan, I. R., Eds.; Special Publication No. 3; The Geochemical Society, 1991; pp 409–422.

(74) Rosso, K. M.; Smith, D.; Dupuis, M. An ab initio model of electron transport in hematite (α-Fe_2O_3) basal planes. *J. Chem. Phys.* **2003**, 6455–6466.

(75) Czurda, K. In *Developments in Clay Science*; Bergaya, F., Theng, B. K. G., Lagaly, G., Eds.; Elsevier, 2006; Vol. Volume 1; Chapter 11.3, pp 693–701.

(76) Seymour, K. J. Landfill Lining for Leachate Containment. *J. Inst. Water Environ. Manage.* **1992**, *6*, 389–396.

(77) Anastacio, A. S.; Aouad, A.; Sellin, P.; Fabris, J. D.; Bergaya, F.; Stucki, J. W. Characterization of a redox-modified clay mineral with respect to its suitability as a barrier in radioactive waste confinement. *Appl. Clay Sci.* **2008**, *39*, 172–179.

(78) Pusch, R. Use of Bentonite for Isolation of Radioactive Waste Products. *Clay Miner.* **1992**, *27*, 353–361.

(79) Pusch, R. In *Developments in Clay Science*; Bergaya, F., Theng, B. K. G., Lagaly, G., Eds.; Elsevier, 2006; Vol. Volume 1; Chapter 11.4, pp 703–716.

(80) Stucki, J. W.; Roth, C. B. Oxidation-reduction mechanism for structural iron in nontronite. *Soil Sci. Soc. Am. J.* **1977**, *41*, 808–814.

(81) Stucki, J. W.; Low, P. F.; Roth, C. B.; Golden, D. C. Effects of oxidation-state of octahedral iron on clay swelling. *Clays Clay Miner.* **1984**, *32*, 357–362.

(82) Stucki, J. W.; Wu, J.; Gan, H. M.; Komadel, P.; Banin, A. Effects of iron oxidation state and organic cations on dioctahedral smectite hydration. *Clays Clay Miner.* **2000**, *48*, 290–298.

(83) Yan, L. B.; Stucki, J. W. Effects of structural Fe oxidation state on the coupling of interlayer water and structural Si-O stretching vibrations in montmorillonite. *Langmuir* **1999**, *15*, 4648–4657.

(84) Bernal, J. D. The Physical Basis of Life. *Proc. Phys. Soc. A* **1949**, *62*, 537.

(85) Brack, A. In *Developments in Clay Science*; Bergaya, F., Theng, B. K. G., Lagaly, G., Eds.; Elsevier, 2006; Vol. Volume 1; Chapter 7.4, pp 379–391.

(86) Meunier, A.; Petit, S.; Cockell, C. S.; El Albani, A.; Beaufort, D. The Fe-Rich Clay Microsystems in Basalt-Komatiite Lavas: Importance of Fe-Smectites for Pre-Biotic Molecule Catalysis During the Hadean Eon. *Orig Life Evol Biosph* **2010**, *40*, 253–272.

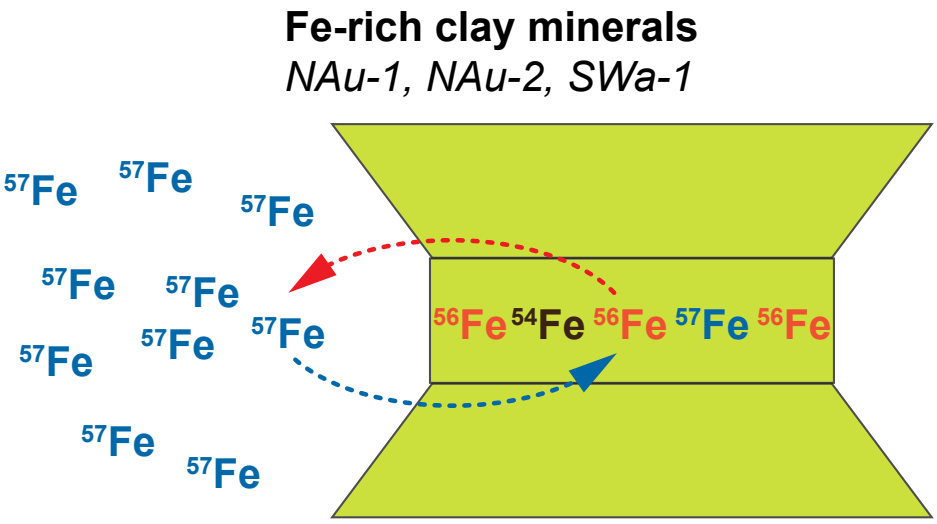
Fe-rich clay minerals
NAu-1, NAu-2, SWa-1
57Fe
57Fe
57Fe
57Fe
57Fe
57Fe
57Fe
57Fe
57Fe
56Fe
54Fe
56Fe
57Fe
56Fe

TOC art